Contact Resistance of Oriented Electroplated Nickel*

Thomas F. Davis
David Kahn
AMP Incorporated

ABSTRACT

The variation of the surface oxidation rate of single-crystal nickel with crystalline orientation is well known and has been studied for some time. A corresponding variation of contact resistance after ambient exposure of single-crystal specimens has been observed in our laboratory and has been duplicated with electroplated nickel having a preferred grain orientation (texture). Data on the contact resistance behavior of separable connectors with electroplate orientation and plating conditions are discussed.

INTRODUCTION

Environmental tests at AMP have shown that test coupons plated with nickel exhibit surprisingly different contact resistance when exposed to the atmosphere for long periods of time. A series of chemical analyses showed that this difference could not be due to the inclusion of metallic or other impurities. Similarly, surface analyses showed that the difference could not be due to any variation in the surface arising from oils or other contaminants.

The only significant difference that could be observed among the various nickel platings was a variation in plating texture. If a polycrystalline metallic film is examined by x-ray diffraction, the peaks corresponding to diffraction from the single-crystal grains in the film with atomic planes parallel to the surface will have certain relative intensities. If the grains have a random orientation, the peak ratios will correspond to those listed in the literature.[1] If the orientation of the grains is not random, then the peak intensity ratios will be different, and the degree of orientation or texture can be determined.

A variation in texture of plated metals with plating conditions is not new and has been known for some time. The variation in texture with current density and pH for a Watts bath is shown in Figure 1a.[2] A similar variation of texture with additive concentration and current density is shown in Figure 1 b.[3]

A variation in contact resistance due to this variation in texture could be understood if the rate of oxidation also depends on the crystalline orientation of the nickel surface. Fortunately, a large amount of work has been done on the oxidation rates in single-crystal nickel, since clean surfaces are easy to obtain and nickel has only one stable oxide.

OXIDATION RATES ON NICKEL SURFACES

Orders of magnitude variation in electrochemical reactions with crystalline orientation have been observed by a number of investigators.[4] This should not be too unexpected since the arrangement of atoms on the surfaces of a face-centered-cubic (fee) crystal like nickel is quite different for various orientations. The arrangement of the atoms on { 100), {110], and {111) surfaces are shown in Figure 2. The {111] planes are referred to as close-packed planes since the atoms are spaced as close together as possible. The { 100) atomic planes are seen to have quite a different atomic arrangement. These planes make up the six surfaces of a fcc unit lattice cell. The { 110} atomic planes consist of rows of closely spaced atoms arranged in a zigzag fashion.

If a single crystal of nickel, ground and electropolished into a sphere, is lightly oxidized in an oven containing a pure

*Presented AESF SUR/FIN '9 1 Conference 24 June 1991, Toronto, Canada,

oxygen atmosphere, interference patterns corresponding to variations in the oxide thickness at various points on the sphere are observed. An example of this type of pattern on a single-crystal sphere of fcc copper is shown in Figure 3.[5] The <111> axes with three-fold symmetry and the< 100> axes with four-fold symmetry are easily seen. These patterns show clearly that differing crystal planes oxidize at different rates.

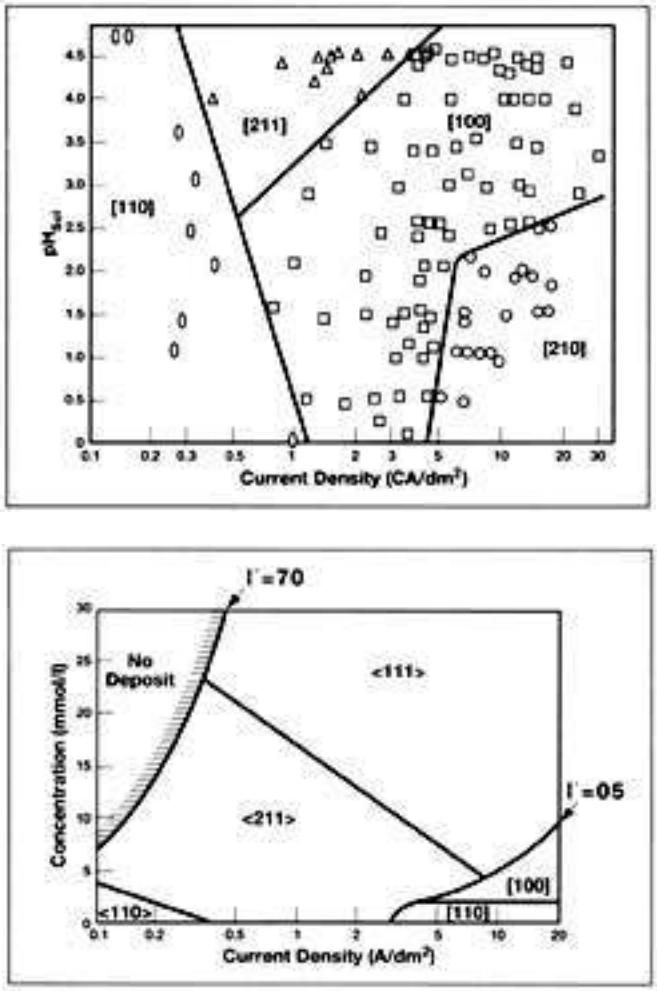

Figure 1. Variation in plating orientation: **a)** with current density and pH for a Watts bath with no brightener;[2] **b)** with concentration of butynediol inhibitor. The parameter **G** is the ratio of the brightener concentration to the current density.[3]

More quantitative work at high temperatures shows that oriented surfaces do oxidize at different rates, and at 600°C in 0.67 Pa oxygen the order of descending oxidation rate is found to be { 100), {1ll], and {112}.[6] These results are shown in Figure 4. Similar results were found by other investigators. [7,8]

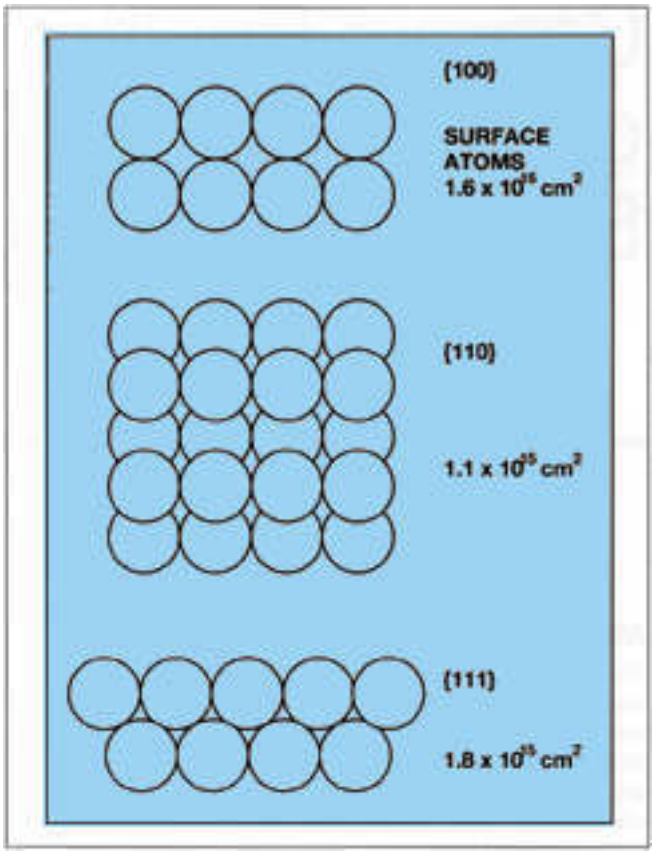

Figure 2. Atom arrangement and surface density on low index planes for an fcc crystal.

Room-temperature results of Kulpa and Frankenthal show an approach to a limiting thickness of about 2.5 nm of oxide for exposure of a sulfamate bath plating at 40°C and 95% relative humidity.[9] This thickness is approximately 12 layers of NiO. The orientation of the plating was not determined. Holloway and Hudson report a saturation thickness of 0.95 nm or 3.94 layers of NiO on a Ni {100 } surface at 302 K (29°C).10 Mitchell *et al.* report that the NiO layer on Ni {100} surfaces grows to a limiting thickness of approximately 6 A (1.5 unit cells), ". . . which does not thicken at room temperatures with additional oxygen exposure."[11] On the other hand, they found that NiO on Ni {110} and Ni {111} surfaces continues to grow logarithmically with continued oxygen exposure at 40°C. [12,13] Norton *et al.* compared the growth rate of NiO at 295 K (22°C) on nickel and found rates in the order Ni(110) > Ni(l11) > Ni(100), but their oxygen exposures were too low to investigate the saturation of oxide thickness. [14]

CONTACT RESISTANCE MEASUREMENTS

None of the oxidation measurements mentioned above included any measurements of the contact resistance. Pinnel et *al.* measured the oxide thickness and the contact resistance for cast nickel coupons. At 50°C, they estimate an

oxide thickness of approximately 5 Å after a 1000-hr exposure to the ambient. During this time the contact resistance *decreased* from about 100 mΩ to about 60 mΩ using a force of 50 g on the probe tip. These results are shown in Figure 5. The nickel coupons were reported to be slightly textured with enhancement of { 100} planes parallel to the sheet surface.[15]

Figure 3. Anisotropic oxidation of a single crystal copper sphere. The fourfold <100> axis and threefold <111> axis can be identified.[5]

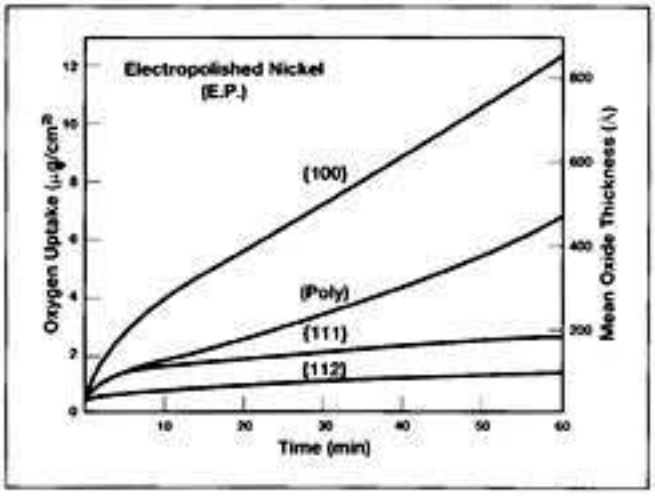

Figure 4. Oxidation rates at 600°C and 5E-03 Torr oxygen for electropolished nickel crystals.[6]

To confirm the theory that the contact-resistance behavior of nickel is dependent on the crystal orientation, single crystals

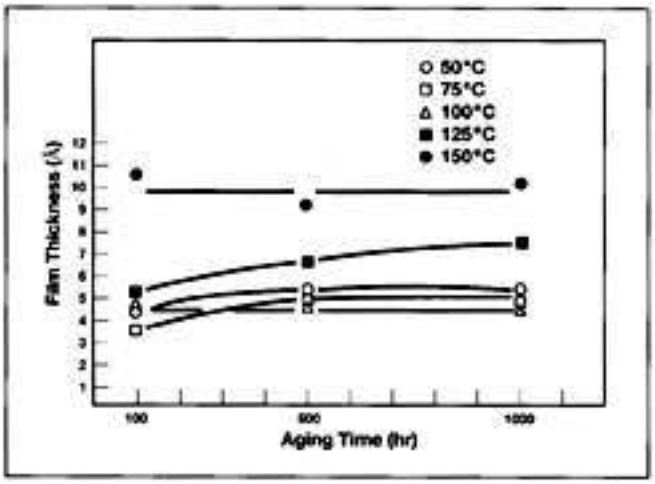

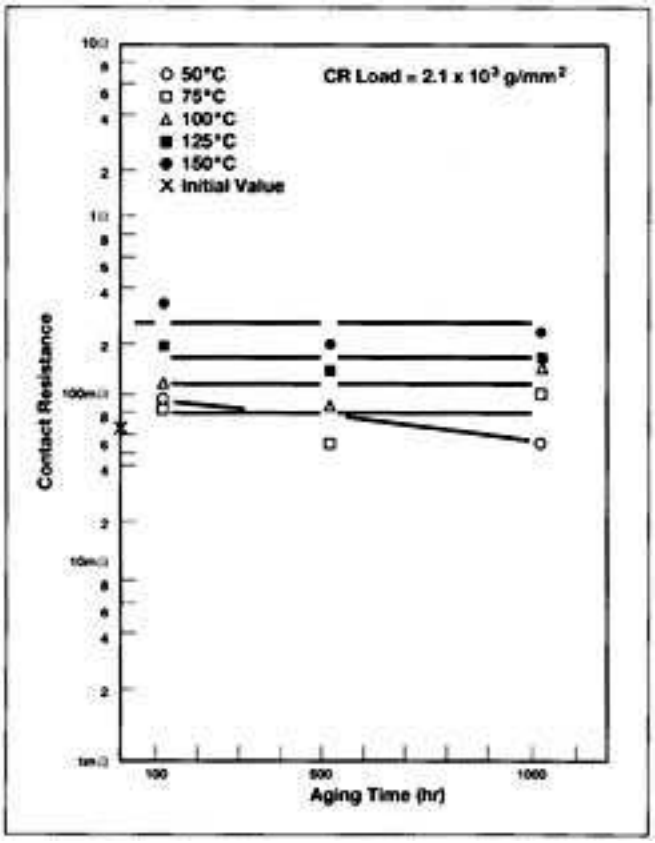

Figure 5a) Film thickness vs. exposure time for electroplated nickel from 50°C to 150°C[15] **b)** Contact resistance vs. exposure time for electroplated nickel from 50°C to 150°C.[15]

Table 1. Plating Condition and Orientation of Nickel-Plated Coupons

Sample	Current Density ASF	Bath pH	Bath Temp. (°C)	Fault Probability (α)	Residual Stress σ (ksi)	(hkl)	X-Ray Integrated Intensity (rel.)	Measured Thickness (μin)
A	15	3.5	30	-7.6×10^{-3}	1.69	111	57	160
						200	100	
						220	5	
						311	13	
						222	4	
						400	6	
B	30	3.5	45	-4.1×10^{-4}	-41.2	111	49	136
						200	100	
						220	4	
						311	10	
						222	3	
						400	6	
C	30	3.5	60	-2.1×10^{-3}	-49.0	111	30	122
						200	100	
						220	2	
						311	6	
						222	2	
						400	6	
D	30	5.5	30	-4.6×10^{-3}	33.2	111	38	161
						200	100	
						220	2	
						311	6	
						222	2	
						400	6	
E	30	5.5	45	-6.2×10^{-3}	-25.7	111	29	159
						200	100	
						220	3	
						311	7	
						222	2	
						400	7	
F	30	5.5	60	-8.2×10^{-4}	-59.4	111	100	149
						200	83	
						220	30	
						311	16	
						222	3	
						400	—	
Random Orientation[1]						111	100	
						200	42	
						220	21	
						311	20	
						222	7	
						400	4	

of pure nickel were obtained. [16] Force/resistance curves were measured on the surfaces, cut from the same single crystal, parallel to the {111], { 110}, and { 100) planes. The force versus contact-resistance curves are shown in Figure 6. These results show a significant difference in the contact resistance that can only be explained by the orientation and its effect on oxide growth.

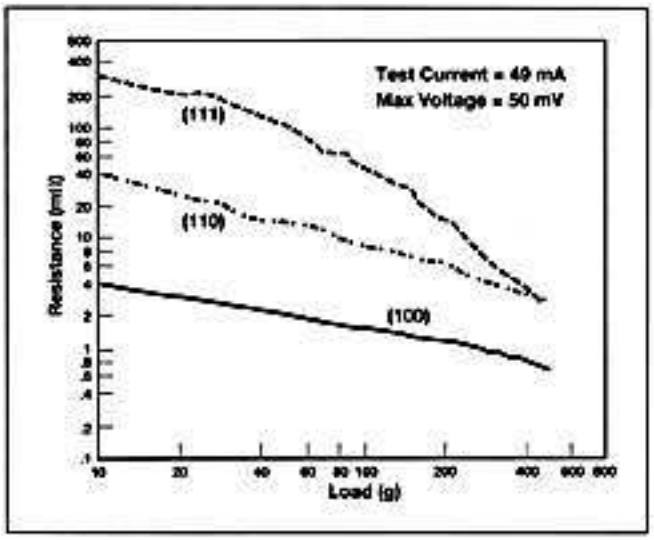

Figure 6. Resistance-force curves for three oriented nickel single-crystal surfaces vs. gold.

Subsequent to this, work was done to determine if good contact resistance could be consistently obtained with polycrystalline electrodeposits, instead of single crystals. A series of samples were produced using a sulfamate nickel plating bath, with varying plating parameters. The observed textures and bath parameters are listed in Table 1. Contact-resistance measurements were then taken in the as-plated condition, as well as after 24 and 72 hours at 150°C. The results for the two samples with the greatest and least amount of { 100) texture are shown in Figures 7 and 8. This work confirmed that polycrystalline electrodeposits would behave similarly to single crystals, as long as a majority of the grains are oriented with the { 100} plane parallel to the surface. This seemingly modest requirement of preferentially oriented crystallite can be understood in the light of contact theory. When two contact surfaces are pressed against each other, they are not in physical contact over a large area but are in actual contact only at a limited number of locations where projecting asperities on the two surfaces touch each other. When a current passes from one surface to the other, it passes only through these submicroscopic locations of actual contact. The remaining portions of the contact surfaces are not a part of the contact area.

In the case of nickel-plated contact surfaces, it must be remembered that the crystallite are quite small and crystallite which have the preferred { 100} orientation will be randomly distributed on both surfaces. When the two surfaces with a { 100) texture are brought into engagement with each other, there is a high probability that a sufficient number of preferentially oriented crystallite on the one surafce will be against preferentially oriented crystallite on the other surface to ensure good contact. These low-resistance contacts will tend to short out any higher-resistance contact spots. Obviously the greater the texture of the deposit, the higher the probability of a contact between asperities having the same orientation.

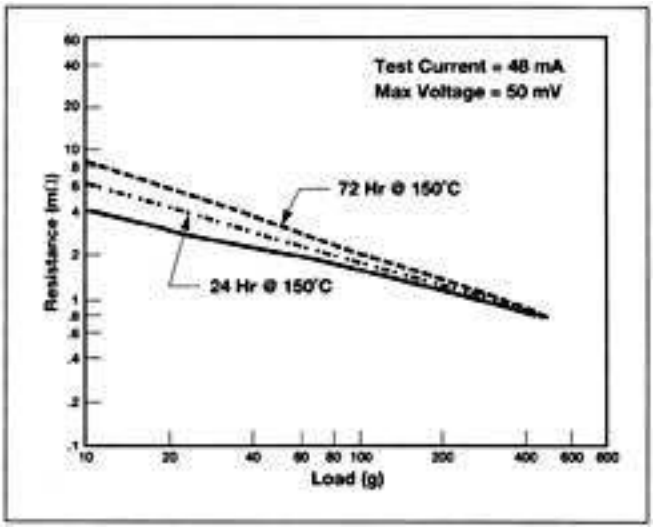

Figure 7. Resistance-force plot for nickel plating sample E as plated, and after heat aging at 150°C for 24 and 72 hours.

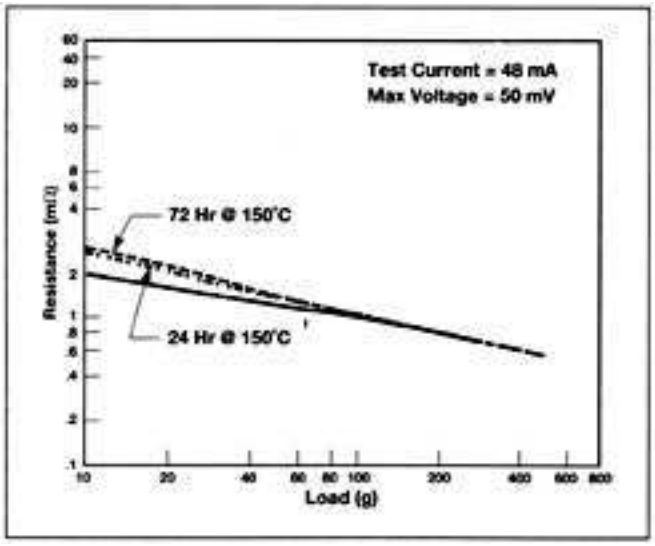

Figure 8. Resistance-force plot for nickel plating sample F as plated, and after heat aging at 150°C for 24 and 72 hours.

PRODUCT TESTING

To evaluate the performance of these platings in connector applications, product testing was initiated.

Test Set A

The aim of the first test was to differentiate the performance of nickel with two different orientations, primarily {111} versus primarily { 100}, in different interconnect technologies.

Test samples, comprising 112 cells of 20 contacts/cell, of the following products were plated:

Product	Interconnect Technology
AMP-LATCH NOVO	Insulation Displacement
AMP Wrap	Wire Wrap
Taper Pins & Receptacles	Force-Fit Pin
AMP Power Leek	High-Force Crimp

Before the samples were terminated, one half were submitted to the following temperature/humidity aging sequence chosen to simulate shelf storage of the product:

64 hours at 85% RH, 85°C

24 hours at dry, 85°C

24 hours at 85% RH, 85°C

32 hours at dry, 85°C

24 hours at 85% RH, 85°C

64 hours at ambient lab conditions.

All samples were then terminated and submitted to the following tests:

Heat Age—Prepared samples were heat-soaked in an oven for 33 days at a temperature of 118°C (244°F) with resistance monitoring occurring initially and after 1,2,4, 8, 16, and 33 days' exposure. Before any resistance measurements were made, the samples were allowed to stabilize at ambient temperature for a minimum of 2 hours.

High Humidity-Prepared samples were subjected to 30 cycles of testing as described in MIL-STD-202E, Method 106D. The temperature change occurred between the extremes of 25°C (77°F) and 65°C (149°F) with an average rate of 16°C (28.8°F) per hour. The test samples were allowed to stabilize at the high temperature for 3 hours, with a relative humidity of 90% to 98% during the temperature rise and during the hold. The relative humidity was maintained at 80% to 98% during the temperature fall. The samples were held at the lower extreme for 8 hours after two high extremes were reached. Thus, each cycle was 24 hours. Electrical resistance measurements were performed initially, and after 10 and 30 cycles. The samples were stabilized at ambient temperature for 2 hours minimum prior to measurement.

The 8-hour hold at the end of each cycle is a modification of the cold shock described in MIL-STD-202E, Method 106D.

Thermal Shock---Samples were prepared and placed in a chamber and subjected to 200 cycles as described in MIL-STD-202E, Method 102, Test Condition D; except that the higher temperature extreme was 105°C. The cycle was as follows:

Step	Temperature	Time
1	–55°C	30 min.
2	25°C	<15 sec.
3	105°C	30min.
4	25°C	<15 sec.

Electrical resistance was monitored at 0,50, 100, and 200 cycles. Samples were stabilized at ambient temperature for 2 hours minimum prior to measurement.

Industrial Mixed Flowing Gas—The samples were exposed to 200 ppb each of H_2S, SO_2 and NO_2 for 800 hours at 40°C with 70% to 80% RH in our flowing gas chamber, EP-716. The samples were measured initially and after exposure times of 100, 200,400, and 800 hours, allowed to sit at ambient temperature for 2 hours minimum, and monitored for contact resistance.

Resistance Measurements—Initially, and at each measurement interval, resistance measurements were taken with our Automatic Resistance Measuring System, EP-381. The system consists of a constant-current source, a digital voltmeter, and a 75-position scanner. The scanner and voltmeter are controlled by a minicomputer. The following sequence describes the technique used to determine each resistance reading:

1. A barrier check is performed with an open-circuit voltage of 20 mV by placing a 0.2-Ω resistor in parallel with the sample using a constant current of 100 mA. Samples with resistance >0.2Ω are recorded as open circuits.

2. The sample is energized with a constant current of 100 mA and forward and reverse voltage measurements are made by reversing the direction of the current.

3. The current is checked every 10 readings by monitoring the voltage drop across a 1. O-Q standard resistor.

4. The resistance is calculated from the expession R = (| Vf | + | Vr |)/21 and stored.

The system is calibrated as a resistance-measuring device once every three months using standard resistors and checked daily for drift with specially-prepared wire lengths mounted on printed circuit boards and kept in a constant-temperature enclosure.

Results

Test results varied depending on the type of interconnect technology. The data is summarized in the ANOME (Analysis of Means) plots presented here. These ANOME plots

present the deviation of the subgroup (i.e. the two orientations) mean change in resistance for each test from the Grand Mean. A negative value indicates a smaller change in resistance and hence indicates better performance.

Insulation Displacement—The only test that showed a significant difference was the heat-age test, where the samples with { 100] orientation performed significantly better. These results are shown in Figure 9a.

Wire Wrap-Samples with { 100] texture were superior to those with {11 1) texture in all tests. Statistical analysis showed that the results were significant (99% confidence level) for the high-humidity, thermal-shock and mixed-flowing-gas tests. These results are shown in Figure 9b.

Force-Fit Pin-Although the results show a slightly better performance of the {111] texture samples, the results are not statistically significant (note change of Y-axis scale). These results are shown in Figure 10a.

High-Force Crimp-The test results showed that the {111} samples were significantly better in the heat-age and mixed-flowing-gas tests. These results are shown in Figure 10b.

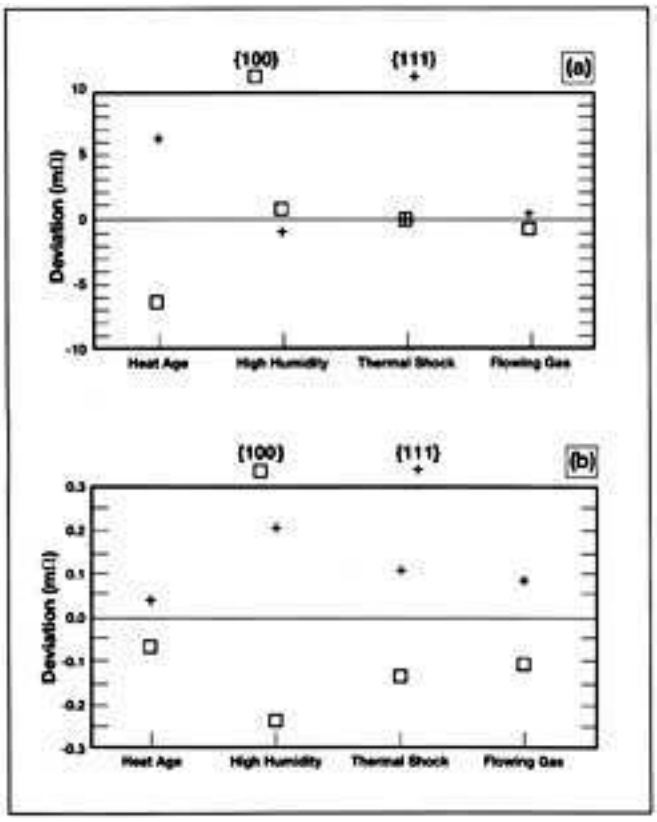

Figure 9. Analysis of means (ANOME) plot of resistance change in oriented nickel plating for a) insulation displacement and b) wire wrap interconnects after testing. A negative value indicates better performance.

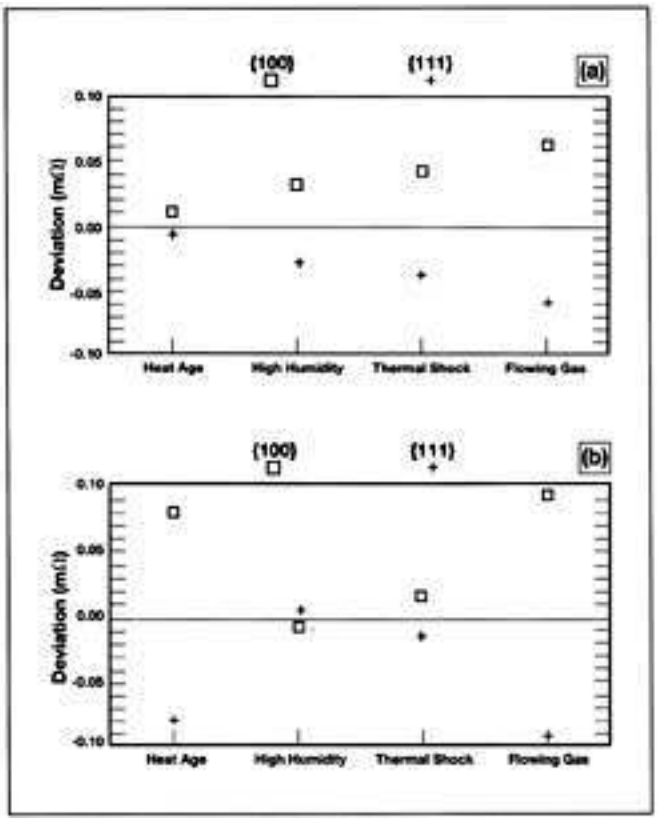

Figure 10. Analysis of means (ANOME) plot of resistance change in oriented nickel plating for a) force-fit pin and b) high-force crimp interconnects after testing. A negative value indicates better performance.

Test Set B

The second test program consisted of an evaluation of the effect of nickel-plated contact orientation on the AMP PACE connector. This connector is a printed circuit board card-edge connector containing three different interconnect technologies: separable contacts, compliant pin, and wire wrap. Two sets of samples of AMP PACE connectors were plated with nickel-one primarily of { 100] orientation, the other of {111] orientation. Also included in the test were control samples of standard AMP PACE product, which are plated with gold-over-nickel in the separable contact area and 93/7 tin/lead in the compliant pin and wire wrap areas.

The samples, 72 cells of 100 contacts/cell, were submitted to the same preconditioning sequence and tests as described above except for the following: the heat-age test temperature was 105°C, and the samples were exposed to the mixed-flowing-gas test for 20 days (480 hours).

This test was considered more significant in that the test program would include a separable contact area, which is generally more susceptible to corrosion; and we are comparing the nickel plate to gold and tin/lead platings, which are the standard platings in our industry. ANOME plots are

shown for the three methods of interconnection. The overall analysis supports the following two hypotheses at the 99% confidence level:

1. That {100] texture platings performed better in the above environmental tests than {111} texture platings.

2. That one or both platings can be used instead of gold or tin/lead under some conditions.

Results of these tests for the various interconnect technologies and environments are:

Card Edge—Nickel {100} texture platings performed significantly better in the heat-age and mixed-flowing-gas tests, and worse in the thermal-shock test in comparison to the Grand Mean. The {100] nickel platings were significantly better than the gold-plated samples in the heat-age test as well. These results are shown in Figure 11.

Compliant Pin-Nickel {100) texture platings performed significantly better in thermal-shock testing, and significantly worse in the high-humidity test. The {100] -oriented nickel platings were significantly better than the tin/lead platings in the thermal-shock test as well. These results are shown in Figure 12a.

Wire Wrap-Nickel {100] plating performed significantly better in heat-age, thermal-shock and mixed-flowing-gas tests. There was no indfference in the results of the high-humidity test. The {100} -oriented platings were slightly worse than the tin/lead platings for all tests. These results are shown in Figure 12b.

To show in more detail the differences in behavior, we have included probability plots of two test cells. Figure 13 is a probability plot of the heat-age test on the card-edge contact area. Data are presented as the change in resistance as a cumulative percentage for the three plating types. Ideal behavior would be a horizontal line. Deviations from this, particularly a significant upward trend, indicate degradation.

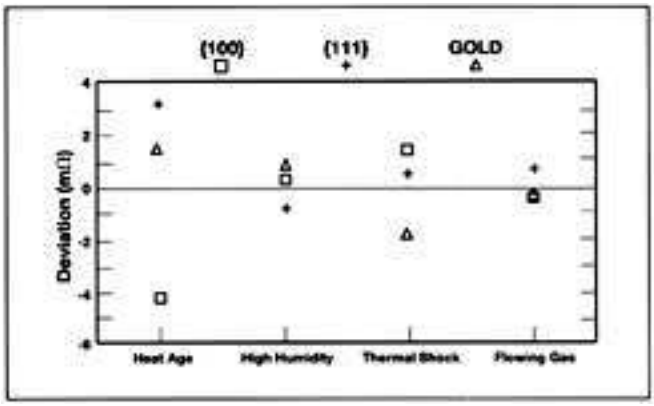

Figure 11. Analysis of means (ANOME) plot of resistance change in oriented nickel and gold plating for a card-edge interconnect. A negative value indicates better performance.

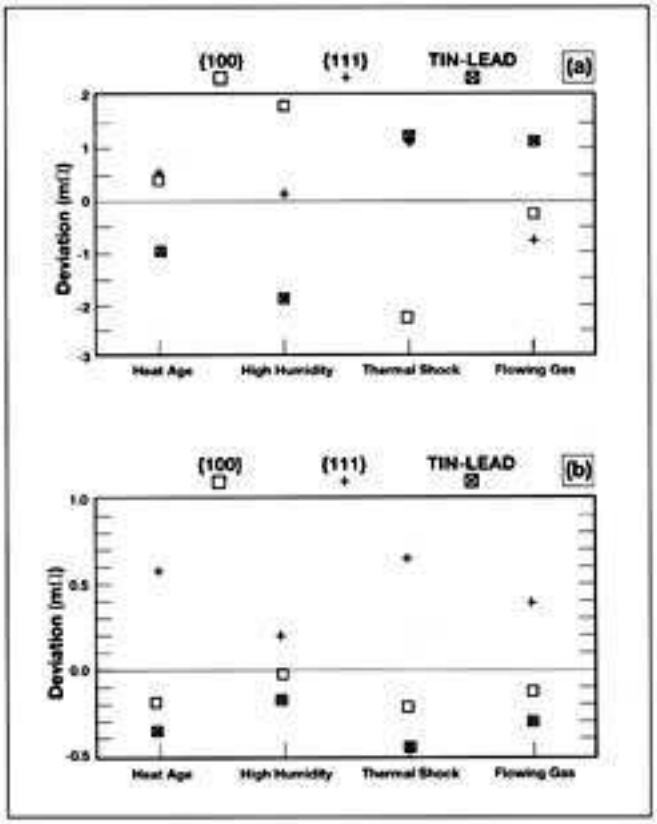

Figure 12. Analysis of means (ANOME) plot of resistance change in oriented nickel and tin-lead plating for an a) compliant pin and b) wire wrap interconnects after testing. A negative value indicates better performance.

As can be seen, nickel with a {100} texture behaves slightly better than gold-plated samples and significantly better than {11 1) textured nickel.

The data in Figure 14 shows the card-edge resistance behavior for shelf-life treated connectors in the mixed-flowing-gas test. Again, {100} texture nickel behaves comparably to gold, and better than {111] texture nickel.

SUMMARY

A large variation in the contact resistance of electroplated nickel coatings at AMP was traced to the variation of grain orientation (texture) in the plating. Platings with predominantly { 100} crystal planes parallel to the plating surface have a significantly lower contact resistance than platings with a {111} texture after a long exposure to ambient air.

The variation in oxidation rate with orientation has been observed in other laboratories at both high and ambient temperatures. In particular, the oxidation of { 100) -oriented nickel single-crystal surfaces was measured to be self-limiting at room temperature. This behavior was also observed at AMP using oriented single-crystal samples.

Product testing of AMP connectors using oriented nickel plating showed that in most cases { 100] -oriented nickel was superior to { 111 }-oriented nickel and that one or both platings can be used instead of gold or tin/lead under some conditions.

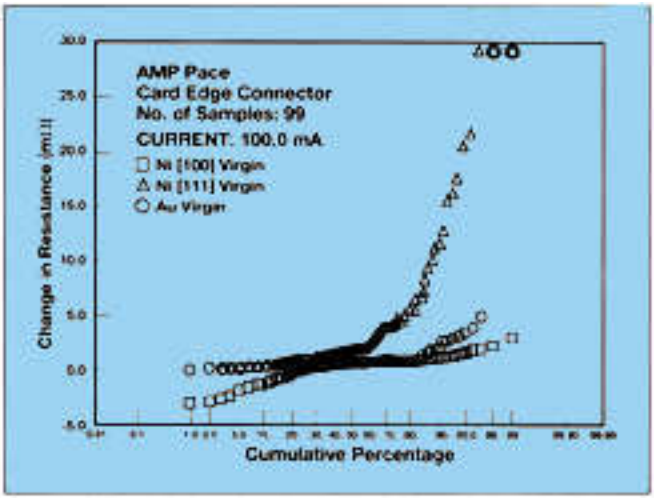

Figure 13. Change in resistance vs. cumulative percentage for {100} Ni, {111} Ni and gold after 103 days heat age.

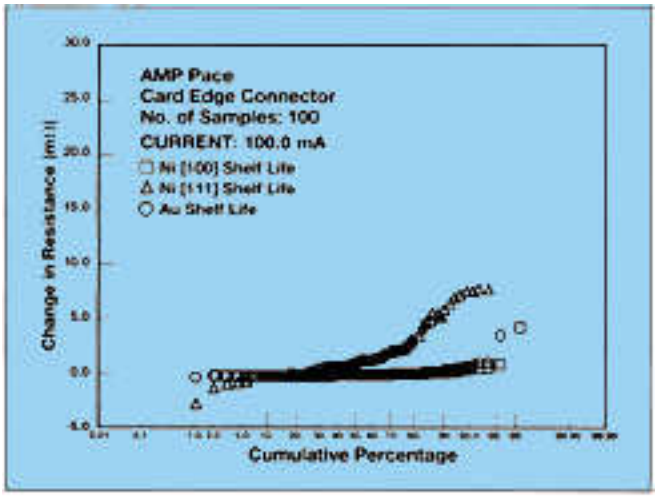

Figure 14. Change in resistance vs. cumulative percentage for {100} Ni, {111} Ni and gold after 20 days industrial-mixed-flowing gas.

REFERENCES

1. JCPDS-International Centre for Diffraction Data, Swarthmore, PA 19081.

2. J. Amblard et *al.*, Oberflache-Surface **18,** 1 (1977).

3. J. Amblard *et al.*, Jour. Appl. Electrochemistry **9,** 233 (1979).

4. E. Yeager, "Single-Crystal Electrochemistry," Annual Conference of the Case Center for Electrochemical Sciences, Case Western Reserve University (1989).

5. C.J. Sparks, "Research with X-rays," *Physics Today* (May, 1981) p. 41.

6. M.J. Graham *et al.*, Jour. Electrochem. Sot. **120** (11), 1523 (1973).

7. J.V. Cathcart *et al.*, Jour. Electrochem. Sot. **116** (5), 664 (1969).

8. D.E. Larsen, Scripts Metallurgic **21,** 1379 (1987).

9. S.H. Kulpa and R.P. Frankenthal, Jour. Electrochem. Soc. **124** (10), 1588 (1977).

10. P.H. Holloway and J.B. Hudson, Surface Science **43,** 123 (1974).

11. D.F. Mitchell *et al.*, Surface Science **61**,355 (1976).

12. D.F. Mitchell et *al.*, Surface Science **69,**310 (1977).

13. D.F. Mitchell and M.J. Graham, Surface Science **114,** 546 (1982).

14. P.R. Norton *et al.*, Surface Science **65,** 13 (1977),

15. M.R. Pinnel *et al.*, Jour. Electrochem. Sot. **126** (7), 1274 (1979).

16. Monocrystals Company, Cleveland, OH 44117.

Thomas F. Davis is an Associate Director in the Technology Group at AMP Incorporated in Harrisburg, Pennsylvania.

Mr. Davis received a B.S. in chemistry from Lehigh University. Since joining AMP in 1983, he has researched various aspects of electrodeposition, including solderability, process control, and bath chemistry. He holds 15 U.S. patents.

David Kahn is a Senior Member of the Technical Staff in the Metal Processing Technology Group at AMP Incorporated in Harrisburg, Pennsylvania.

Dr. Kahn received a B.S. in engineering physics from the University of Illinois and a Ph.D. in physics from the University of Chicago. He was subsequently employed at the Lewis Laboratory of NASA and the Martin Marietta Research Laboratory. Since joining AMP, he has worked in the areas of transition metal compounds, electrical contact oxidation and stress relaxation, the characterization of metal platings, and multivariate analysis of plating systems.

射 频 和 天 线 设 计 培 训 课 程 推 荐

易迪拓培训(www.edatop.com)由数名来自于研发第一线的资深工程师发起成立，致力并专注于微波、射频、天线设计研发人才的培养；我们于 2006 年整合合并微波 EDA 网(www.mweda.com)，现已发展成为国内最大的微波射频和天线设计人才培养基地，成功推出多套微波射频以及天线设计经典培训课程和 ADS、HFSS 等专业软件使用培训课程，广受客户好评；并先后与人民邮电出版社、电子工业出版社合作出版了多本专业图书，帮助数万名工程师提升了专业技术能力。客户遍布中兴通讯、研通高频、埃威航电、国人通信等多家国内知名公司，以及台湾工业技术研究院、永业科技、全一电子等多家台湾地区企业。

易迪拓培训课程列表：http://www.edatop.com/peixun/rfe/129.html

射频工程师养成培训课程套装

该套装精选了射频专业基础培训课程、射频仿真设计培训课程和射频电路测量培训课程三个类别共 30 门视频培训课程和 3 本图书教材；旨在引领学员全面学习一个射频工程师需要熟悉、理解和掌握的专业知识和研发设计能力。通过套装的学习，能够让学员完全达到和胜任一个合格的射频工程师的要求…

课程网址：http://www.edatop.com/peixun/rfe/110.html

ADS 学习培训课程套装

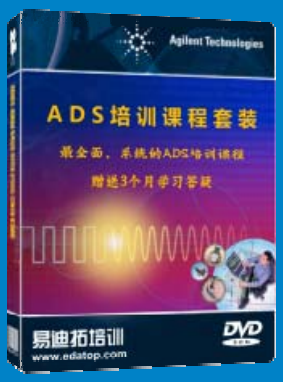

该套装是迄今国内最全面、最权威的 ADS 培训教程，共包含 10 门 ADS 学习培训课程。课程是由具有多年 ADS 使用经验的微波射频与通信系统设计领域资深专家讲解，并多结合设计实例，由浅入深、详细而又全面地讲解了 ADS 在微波射频电路设计、通信系统设计和电磁仿真设计方面的内容。能让您在最短的时间内学会使用 ADS，迅速提升个人技术能力，把 ADS 真正应用到实际研发工作中去，成为 ADS 设计专家...

课程网址： http://www.edatop.com/peixun/ads/13.html

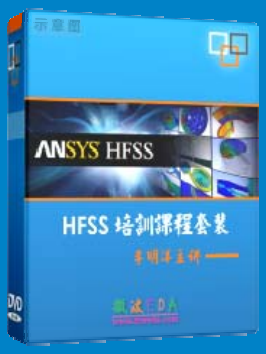

HFSS 学习培训课程套装

该套课程套装包含了本站全部 HFSS 培训课程，是迄今国内最全面、最专业的 HFSS 培训教程套装，可以帮助您从零开始，全面深入学习 HFSS 的各项功能和在多个方面的工程应用。购买套装，更可超值赠送 3 个月免费学习答疑，随时解答您学习过程中遇到的棘手问题，让您的 HFSS 学习更加轻松顺畅…

课程网址：http://www.edatop.com/peixun/hfss/11.html

CST 学习培训课程套装

该培训套装由易迪拓培训联合微波 EDA 网共同推出，是最全面、系统、专业的 CST 微波工作室培训课程套装，所有课程都由经验丰富的专家授课，视频教学，可以帮助您从零开始，全面系统地学习 CST 微波工作的各项功能及其在微波射频、天线设计等领域的设计应用。且购买该套装，还可超值赠送 3 个月免费学习答疑…

课程网址：http://www.edatop.com/peixun/cst/24.html

HFSS 天线设计培训课程套装

套装包含 6 门视频课程和 1 本图书，课程从基础讲起，内容由浅入深，理论介绍和实际操作讲解相结合，全面系统的讲解了 HFSS 天线设计的全过程。是国内最全面、最专业的 HFSS 天线设计课程，可以帮助您快速学习掌握如何使用 HFSS 设计天线，让天线设计不再难…

课程网址：http://www.edatop.com/peixun/hfss/122.html

13.56MHz NFC/RFID 线圈天线设计培训课程套装

套装包含 4 门视频培训课程，培训将 13.56MHz 线圈天线设计原理和仿真设计实践相结合，全面系统地讲解了 13.56MHz 线圈天线的工作原理、设计方法、设计考量以及使用 HFSS 和 CST 仿真分析线圈天线的具体操作，同时还介绍了 13.56MHz 线圈天线匹配电路的设计和调试。通过该套课程的学习，可以帮助您快速学习掌握 13.56MHz 线圈天线及其匹配电路的原理、设计和调试…

详情浏览：http://www.edatop.com/peixun/antenna/116.html

我们的课程优势：

※ 成立于 2004 年，10 多年丰富的行业经验，

※ 一直致力并专注于微波射频和天线设计工程师的培养，更了解该行业对人才的要求

※ 经验丰富的一线资深工程师讲授，结合实际工程案例，直观、实用、易学

联系我们：

※ 易迪拓培训官网：http://www.edatop.com

※ 微波 EDA 网：http://www.mweda.com

※ 官方淘宝店：http://shop36920890.taobao.com